The Astrophysical Journal, 925:40 (9pp), 2022 January 20 https://doi.org/10.3847/1538-4357/ac36da

The Relativistic Jet and Central Engine of Fermi Blazars

Hubing Xiao[1], Zhihao Ouyang[2], Lixia Zhang[3,4,5], Liping Fu[1], Shaohua Zhang[1], Xiangtao Zeng[3,4,5], and Junhui Fan[3,4,5]
[1] Shanghai Key Lab for Astrophysics, Shanghai Normal University Shanghai, 200234, People's Republic of China
[2] School of Physics and Materials Science, Guangzhou University Guangzhou, 510006, People's Republic of China
[3] Center for Astrophysics, Guangzhou University Guangzhou, 510006, People's Republic of China; hubing.xiao@shnu.edu.cn
[4] Key Laboratory for Astronomical Observation and Technology of Guangzhou Guangzhou 510006, People's Republic of China
[5] Astronomy Science and Technology Research Laboratory of Department of Education of Guangdong Province Guangzhou, 510006, People's Republic of China
fjh@gzhu.edu.cn
Received 2021 August 17; revised 2021 October 25; accepted 2021 November 1; published 2022 January 24

Abstract

The origin of jets is one of the most important issues concerning active galactic nuclei, yet it has remained obscure. In this work, we made use of information from emission lines, spectral energy distributions, and Fermi–LAT γ-ray emission to construct a blazar sample that contains 667 sources. We note that jet power originations are different for BL Lacertae objects (BL Lacs) and flat-spectrum radio quasars (FSRQs). The correlation between jet power $P_{\rm jet}$ and the normalized disk luminosity $L_{\rm Disk}/L_{\rm Edd}$ shows a slope of -1.77 for BL Lacs and a slope of 1.16 for FSRQs. The results seem to suggest that BL Lac jets are powered by extracting black hole (BH) rotation energy, while FSRQ jets are mostly powered by accretion disks. Meanwhile, we find the accretion ratio $\dot{M}/\dot{M}_{\rm Edd}$ increases with the normalized γ-ray luminosity. Based on this, we propose a dividing line, $\log(L_{\rm BLR}/L_{\rm Edd}) = 0.25\log(L_\gamma/L_{\rm Edd}) - 2.23$, to separate FSRQs and BL Lacs in the diagram of $L_{\rm BLR}/L_{\rm Edd}$ against $L_\gamma/L_{\rm Edd}$ using a machine-learning method; the method gives an accuracy of 84.5%. In addition, we propose an empirical formula, $M_{\rm BH}/M_\odot \simeq L_\gamma^{0.65}/21.46$, to estimate BH mass based on a strong correlation between γ-ray luminosity and BH mass. Strong γ-ray emission is typical in blazars, and the emission is always boosted by a Doppler-beaming effect. In this work, we generate a new method to estimate a lower limit of Doppler factor δ and give $\delta_{\rm BL\ Lac} = 7.94$ and $\delta_{\rm FSRQ} = 11.55$.

Unified Astronomy Thesaurus concepts: Blazars (164); Flat-spectrum radio quasars (2163); BL Lacertae objects (158); Active galactic nuclei (16); Jets (870)

Supporting material: machine-readable tables

1. Introduction

Active galactic nuclei (AGNs) are the most energetic and persistent extragalactic objects in the universe. Blazars exhibit extreme observation properties, including rapid and high-amplitude variability, high and variable polarization, strong and variable γ-ray emissions, and apparent superluminal motions (Wills et al. 1992; Urry & Padovani 1995; Fan 2002; Fan et al. 2004; Kellermann et al. 2004; Rani et al. 2013; Fan et al. 2014; Lyutikov & Kravchenko 2017; Xiao et al. 2019). These extreme observational properties result from the Doppler-beaming effect caused by relativistic jets (Xiao et al. 2015; Pei et al. 2016; Fan et al. 2017).

Blazars, typically, are hosted by elliptical galaxies and powered by their central supermassive black holes (Urry et al. 2000; Shaw et al. 2012). The broadband spectral energy distribution (SED) of blazar forms a two-hump structure in which the lower energy bump is explained by the synchrotron mechanism and the higher energy bump is attributed to inverse Compton (IC) scattering in a leptonic scenario.

There are two subclasses of blazars that are characterized based on the emission-line strength of optical spectra, namely BL Lacertae objects (BL Lacs) and flat-spectrum radio quasars (FSRQs). The former one characterizes a spectrum with no or weak emission lines (rest-frame equivalent width, EW $< 5\,\mathring{A}$), while the latter one shows strong emission-line features of EW $\geqslant 5\,\mathring{A}$ (Urry & Padovani 1995; Scarpa & Falomo 1997). However, an arbitrary classification based on EW is inadequate. On one hand, a Doppler-boosted nonthermal continuum could swap out spectral emission lines (Blandford & Rees 1978; Xiong & Zhang 2014). On the other hand, EW greater than $5\,\mathring{A}$ may be the result of a particular low state of jet activity. Other indicators have been proposed to divide blazars into subclasses. Ghisellini et al. (2011) and Sbarrato et al. (2012) suggested a distinction of accretion ratio based on the luminosity of broad-line region (BLR) measured in Eddington units, $L_{\rm BLR}/L_{\rm Edd} \sim 10^{-3}$ or $L_{\rm BLR}/L_{\rm Edd} \sim 5\times10^{-4}$, to separate FSRQs and BL Lacs. Abdo et al. (2010a) and Fan et al. (2016) used synchrotron peak frequency ($\log\nu_s$) to divide blazars into low-synchrotron-peaked blazars (LSPs), intermediate-synchrotron-peaked blazars (ISPs), and high-synchrotron-peaked blazars (HSPs), and got compatible results of separating boundaries.

Emission lines with FWHM greater than 1000 km s^{-1} are called broad emission lines; others are known as narrow emission lines. The broad emission lines are employed to estimate the central black hole (BH) mass ($M_{\rm BH}$) by using BLR distance and FWHM assuming the BLR clouds being gravitationally bound by the central BH. The BLR distance can be interpreted through an empirical relation between BLR distance and ionizing luminosity or through reverberation mapping (Wandel et al. 1999; Kaspi et al. 2000, 2005). The reverberation mapping method requires continuous observations on both continuum- and emission-line variations, and gives a more accurate BLR distance than distance–luminosity correlation. Kaspi et al. (2000) calibrated the empirical distance–luminosity correlation by using a reverberation-mapped sample

and got $R_{\rm BLR} \propto L_{5100}^{0.7}$, where L_{5100} is the continuum luminosity at $\lambda = 5100\,\mathring{A}$. Greene & Ho (2005) noted that the emission-line luminosities of Hα and Hβ have a strong correlation with L_{5100}. They substituted the L_{5100} with $L_{\rm H\alpha}$ and $L_{\rm H\beta}$, and suggested $M_{\rm BH} \propto L_{\rm H\alpha}^{0.55}$ and $M_{\rm BH} \propto L_{\rm H\beta}^{0.56}$. Mg II and C IV were also explored by other researchers (McLure & Dunlop 2004; Vestergaard & Peterson 2006; Vestergaard & Osmer 2009; Shen et al. 2011; Shaw et al. 2012). For some sources without broad emission lines, especially BL Lac objects, their $M_{\rm BH}$ can be estimated from the properties of their host galaxies with $M_{\rm BH} - \sigma_\star$ and $M_{\rm BH} - L$, where $\sigma_\star$ and L are the stellar-velocity dispersion and the bulge luminosity (Woo & Urry 2002; Sbarrato et al. 2012; Xiong & Zhang 2014).

The luminosity of the broad-line region ($L_{\rm BLR}$) derived from broad emission lines (Francis et al. 1991; Celotti et al. 1997; Sbarrato et al. 2012), is a good estimator of the power of the accretion disk, $L_{\rm Disk} \simeq 10 L_{\rm BLR}$ (Calderone et al. 2013) because the emission lines are produced by gas that is photoionized by the disk emission. Thanks to Fermi–LAT, we have come to a new era of blazar research. The Fermi collaboration has released four generations of γ-ray source catalogs. The fourth one (4FGL) contains 5064 sources above 4σ signification; among these sources, more than 3130 of identified or associated sources are active galaxies of blazar class (including uncertain-type blazars, BCUs; Abdollahi et al. 2020). Blazars are strong γ-ray emitters; their γ-ray emissions dominate the bolometric luminosity ($L_{\rm jet}^{\rm bol}$) of jets. Thus, L_γ often takes the place of $L_{\rm jet}^{\rm bol}$ in previous research (Ghisellini et al. 2014; Xiong & Zhang 2014; Zhang et al. 2020). The relativistic jets transport energy and momentum from AGNs to large scales, but the jet formation remains unclear. The current theoretical models consider that a jet originates either from the accretion disk and is powered by accretion or from the central BH and is powered by extracting rotation energy (Blandford & Znajek 1977; Blandford & Payne 1982).

The connection between a relativistic jet and an accretion disk has been explored by many authors through studies of γ-ray luminosity, broad emission lines, and black hole mass. Sbarrato et al. (2012) studied blazars that have been detected by Fermi–LAT and that are present in the Sloan Digital Sky Survey (SDSS), suggesting that $L_{\rm BLR}$ correlates well with L_γ. The correlation proves that emission-line photons play a role in producing high-energy γ-rays and points out a clue in the relation between accretion ratio and jet power. The correlations between intrinsic γ-ray luminosity and BH mass, Eddington ratio, and broad-line luminosity were studied by Xiong & Zhang (2014) and Zhang et al. (2020), and they all show positive correlations. A correlation of $\log L_{\rm BLR} \sim (0.98 \pm 0.07) \log P_{\rm jet}$ suggests that jets are powered by extraction from both accretion and BH spin (Xiong & Zhang 2014).

In this work, we focus on the study of the correlations between γ-ray emission and BH mass, relativistic jet related quantities to investigate the jet origination and accretion rate of blazars.

This paper is arranged as follows: in Section 2, we present the samples, the data reduction and results are in Section 3, Section 4 contains our discussion, and our conclusion is in Section 5. The cosmological parameters $H_0 = 73\,{\rm km \cdot s^{-1} \cdot Mpc^{-1}}$, $\Omega_{\rm m} = 0.3$ and $\Omega_\Lambda = 0.7$ have been adopted throughout this paper.

2. The Samples

We collect broad emission-line profiles and BH mass from Paliya et al. (2021), which contains 674 sources. In addition, Paliya et al. (2021) included 10 sources with emission-line parameters or BH mass values from the literature (Baldwin et al. 1981; Chen et al. 2015) and we also used these sources in our work. The classification of Fermi sources are sometimes changed after a new data release. According to the latest classification, there were 17 sources excluded from the blazar class, which gives us a final sample of 667 sources (56 BCUs, 52 BL Lacs, and 559 FSRQs). Meanwhile, we collect the γ-ray flux from 4FGL for the sources in our sample. At last, we cross correlate the sample with Nemmen et al. (2012), Ghisellini et al. (2014), and Tan et al. (2020) to get the entire jet power ($P_{\rm jet}$), the nonthermal radiation power ($P_{\rm rad}$), and the accretion disk luminosity ($L_{\rm Disk}$).

2.1. γ-Ray Luminosity

The SED of the blazar is characterized by two broad bumps, peaking in the millimeter–UV and the megaelectron volt–gigaelectron volt γ-ray bands separately. The emission of the high-energy bump is usually the dominant component for blazars, called a higher Compton dominance that is quantified by $L_{\rm IC}/L_{\rm syn}$, except for some low-power BL Lacs. Thus, the γ-ray luminosity is believed to be a representative of blazar nonthermal bolometric luminosity (Ghisellini et al. 2014; Xiong & Zhang 2014; Zhang et al. 2020). An isotropic γ-ray luminosity is expressed as

$$L_\gamma = 4\pi d_{\rm L}^2 (1+z)^{\alpha_{\rm ph}-2} F, \tag{1}$$

where $d_{\rm L} = (1+z) \cdot \frac{c}{H_0} \cdot \int_1^{1+z} \frac{1}{\sqrt{\Omega_{\rm M} x^3 + 1 - \Omega_{\rm M}}} dx$, z is redshift, $(1+z)^{\alpha_{\rm ph}-2}$ represents a K-correction, $\alpha_{\rm ph}$ is the γ-ray photon index, and F is the γ-ray flux in units of ${\rm erg \cdot cm^{-2} \cdot s^{-1}}$. We calculated L_γ for these 637 sources with available redshift from the NASA/IPAC Extragalactic Database (NED) via Equation (1). The redshift, 4FGL γ-ray photon density and photon spectral index are listed in columns (3), (4), and (6) of Table 1.

2.2. BH Mass and BLR Luminosity

Paliya et al. (2021) obtained emission-line (Hα, Hβ, Mg II, and C IV) luminosity and corresponding continuum luminosity by analyzing optical spectra from SDSS-DR16 data. Continuum luminosity L_λ at 5100 Å is estimated from Hβ luminosity, at 3000 Å is estimated from Mg II luminosity, and at 1350 Å is estimated form C IV luminosity via empirical relations. Then, a virial $M_{\rm BH}$ is estimated through an empirical formula:

$$\log M_{\rm BH} = a + b \log L_\lambda + 2 \log {\rm FWHM}, \tag{2}$$

where $M_{\rm BH}$ in units of solar mass $M_\odot$, L_λ in units of $10^{44}\,{\rm erg \cdot cm^{-2} \cdot s^{-1}}$, FWHM in units of ${\rm km \cdot s^{-1}}$, and the calibration coefficients a and b are taken from McLure & Dunlop (2004), Vestergaard & Peterson (2006), and Shen et al. (2011). The BH mass are listed in column (11) of Table 1.

Moreover, one can infer the luminosity of the entire broad emission-line region ($L_{\rm BLR}$) from the emission-line luminosity. Celotti et al. (1997) calculated $L_{\rm BLR}$ by scaling strong emission lines to the quasar template spectrum of Francis et al. (1991). They set Lyα as a reference flux that contributed to 100; the relative weight of Hα, Hβ, MgII, and C IV lines to 77, 22, 34, and 63; and total broad-line flux was fixed at 556. The BLR

Table 1
Optical and γ-Ray Parameters

4FGL name (1)	Class (2)	z (3)	F_γ (4)	Unc_F_γ (5)	$\Gamma_{\rm ph}$ (6)	$\log L_{\rm H\alpha}$ (7)	$\log L_{\rm H\beta}$ (8)	$\log L_{\rm Mg\ II}$ (9)	$\log L_{\rm C\ IV}$ (10)	$\log M_{\rm BH}/M_\odot$ (11)
J0001.5+2113	F	1.106	1.36E-09	6.86E-11	2.66	42.942 ± 0.016	42.029 ± 0.054	42.503 ± 0.032		7.54 ± 0.07
J0004.3+4614	F	1.81	2.41E-10	3.92E-11	2.58				44.126 ± 0.031	8.36 ± 0.1
J0004.4-4737	F	0.88	4.36E-10	3.75E-11	2.37			42.885 ± 0.099		8.28 ± 0.27
J0006.3-0620	B	0.346676	1.40E-10	3.13E-11	2.13	42.782 ± 0.189	42.004 ± 0.227			8.93 ± 0.4
J0010.6+2043	F	0.5978	1.73E-10	3.44E-11	2.32		43.047 ± 0.048	43.027 ± 0.017		7.86 ± 0.04

Note. Column definitions: (1) 4FGL name; (2) classification: "B" stands for BL Lacs, "F" stands for FSRQs, "U" stands for BCUs; (3) redshift; (4) integral photon flux from 1 to 100 GeV, in units of photon $\cdot$ cm^{-2} $\cdot$ s^{-1}; (5) 1σ error of F_γ; (6) photon index; (7) luminosity of Hα emission line, in units of erg $\cdot$ s^{-1} $\cdot$ cm^{-2}; (8) luminosity of Hβ emission line in units of erg $\cdot$ s^{-1} $\cdot$ cm^{-2}; (9) luminosity of Mg II emission line in units of erg $\cdot$ s^{-1} $\cdot$ cm^{-2}; (10) luminosity of C IV emission line in units of erg $\cdot$ s^{-1} $\cdot$ cm^{-2}; (11) BH mass, in units of solar mass. Only five objects are presented here; the table is available in its entirety in machine-readable form.

(This table is available in its entirety in machine-readable form.)

Table 2
Jet Parameters

4FGL name (1)	Class (2)	z (3)	$\log P_{\rm rad}$ (4)	$\log P_{\rm jet}$ (5)	$\log L_{\rm Disk}$ (SED) (6)	Ref. (7)	$\delta^{\rm L18}$ (8)	$\delta^{\rm Z20}$ (9)	δ (10)
J0001.5+2113	F	1.106						40.77	
J0004.3+4614	F	1.81					7.75	5.63	
J0004.4-4737	F	0.88	44.64	45.88	45.32	G14		10.50	11.92
J0006.3-0620	B	0.346676					6.96	2.48	
J0010.6+2043	F	0.5978					6.02	2.92	

Note. Column definitions: (1) 4FGL name; (2) classification, "B" stands for BL Lacs, "F" stands for FSRQs, "U" stands for BCUs; (3) redshift; (4) jet radiation power, in units of erg $\cdot$ s^{-1}; (5) jet entire power, in units of erg $\cdot$ s^{-1}; (6) luminosity of accretion disk, in units of erg $\cdot$ s^{-1} $\cdot$ cm^{-2}; (7) references of $P_{\rm rad}$, $P_{\rm jet}$, and $L_{\rm Disk}$, that "G14" sands for Ghisellini et al. (2014) and "T20" stands for Tan et al. (2020); (8) Doppler factor from Liodakis et al. (2018); (9) estimated Doppler factor using the method proposed in Zhang et al. (2020); (10) estimated lower-limit Doppler factor in the present work. Only 5 objects are presented here, the table is available in its entirety in machine-readable form.

(This table is available in its entirety in machine-readable form.)

luminosity is, then, expressed as

$$L_{\rm BLR} = \sum_i L_i \cdot \frac{\langle L_{\rm BLR,rel}\rangle}{\sum_i L_{i,\rm rel}}, \quad (3)$$

where $\langle L_{\rm BLR,rel}\rangle = 556$, L_i is observed line luminosity, and $L_{i,\rm rel}$ is relative line luminosity.

2.3. Jet Power

The entire power of a jet ($P_{\rm jet}$) generally contains two types of energy, namely radiation power ($P_{\rm rad}$) and kinetic power ($P_{\rm kin}$), which are in charge of its nonthermal radiation and its propagation.

There are methods to estimate $P_{\rm kin}$, $P_{\rm rad}$, and $P_{\rm jet}$. Cavagnolo et al. (2010) searched for X-ray cavities in different systems including giant elliptical galaxies and cD galaxies and estimated the required jet power that is able to inflate these cavities or bubbles, obtaining a correlation between "cavity" power and radio luminosity,

$$P_{\rm cav} \approx 5.8 \times 10^{43} \left(\frac{P_{\rm radio}}{10^{40}\ {\rm erg \cdot s^{-1}}}\right)^{0.7} {\rm erg \cdot s^{-1}}, \quad (4)$$

and assuming $P_{\rm kin} = P_{\rm cav}$. The radiation power is expressed as

$$P_{\rm rad} = 2f \frac{\Gamma^2 L_{\rm jet}^{\rm bol}}{\delta^4}, \quad (5)$$

where the factor 2 counts for two-sided jets, f equals 16/5 for the case of radiation power consuming through the SSC process. For the case of the EC process, $f = 4/3$ and we replace δ^4 with $\delta^4(\delta/\Gamma)^2$. Two assumptions, $L_{\rm bol}^{\rm jet}$ is represented by L_γ and $\Gamma = \delta$, are both held for blazars (Ghisellini & Tavecchio 2010; Ghisellini et al. 2014; Xiong & Zhang 2014; Zhang et al. 2020).

The $P_{\rm rad}$ and $P_{\rm jet}$ are obtainable through broadband SED fitting. Assuming that the jet power is carried by relativistic electrons, cold protons, the magnetic field, and radiation, the jet power is expressed as

$$P_{\rm jet} = \sum_i \pi R^2 \Gamma^2 c U_i, \quad (6)$$

where $U_i (i = e, p, B, rad)$ are the energy densities associated with an emitting electron $U_{\rm e}$, cold proton $U_{\rm p}$, magnetic field $U_{\rm B}$, and radiation $U_{\rm rad}$ measured in the comoving frame (Ghisellini & Tavecchio 2010; Tan et al. 2020). We collect $P_{\rm rad}$ and $P_{\rm jet}$ from Ghisellini et al. (2014) and Tan et al. (2020) for our sources and list them in columns (4) and (5) of Table 2.

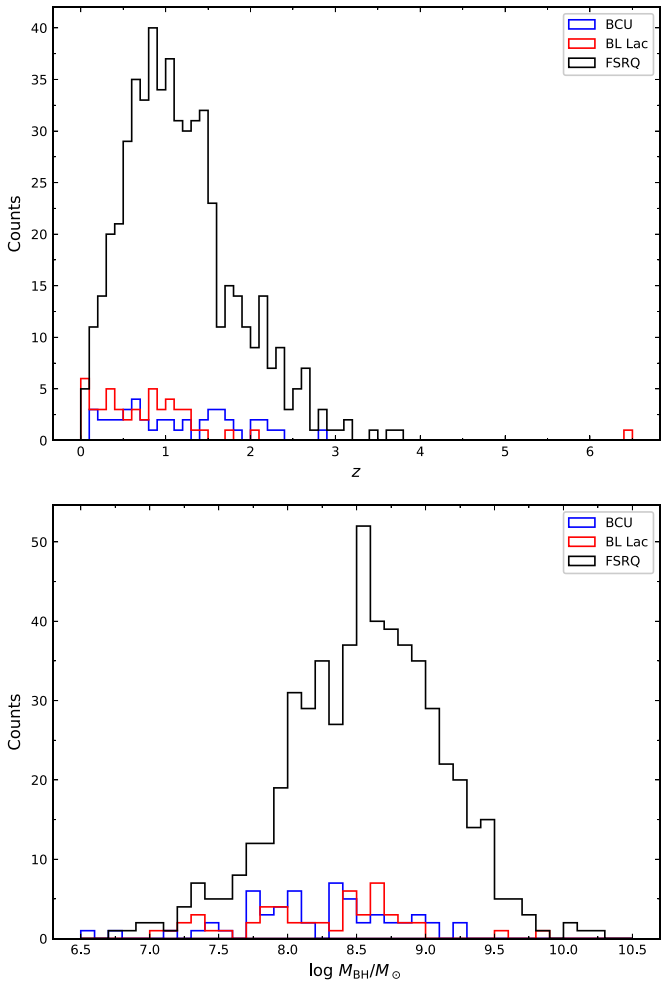

Figure 1. The distributions of redshift (upper panel) and BH mass (lower panel) for the blazars of this work. The blue histogram stands for BCU, the red one stands for BL Lac, and the black one stands for FSRQ, respectively.

3. Results

3.1. The Distributions

The redshift and BH mass distributions of various classes of sources are shown in Figure 1. The redshift, which is obtained by checking their associated names (from 4FGL) in the NED, distributes from 0.00085 to 6.443 with a mean value of 1.147 ± 0.688 for all the blazars in our sample. The mean redshifts for FSRQs is 1.178 ± 0.652, for BL Lacs is 0.697 ± 0.479 (4FGL J0823.3+2224 is excluded for the extremely high redshift 6.443), and for BCUs is 1.144 ± 0.698. The BH mass ranges from 6.35 to 10.2 with a mean value of 8.50 ± 0.58 for all the blazars in our sample. The mean BH masses for FSRQs is 8.56 ± 0.55, for BL Lacs is 8.18 ± 0.66, and for BCUs is 8.19 ± 0.57.

3.2. Correlation between γ-Ray Luminosity and BH Mass

Figure 2 shows BH mass as a function of γ-ray luminosity. We have three sources with debatable γ-ray luminosity due to their redshift; these sources are not shown in Figure 2 and the luminosity of these three sources will not be employed during our analysis throughout this paper. Two (4FGL J1434.2+4204 and 4FGL J2134.2-0154) of them have at least two orders of magnitude lower γ-ray luminosity ($\log L_\gamma = 39.92$ and

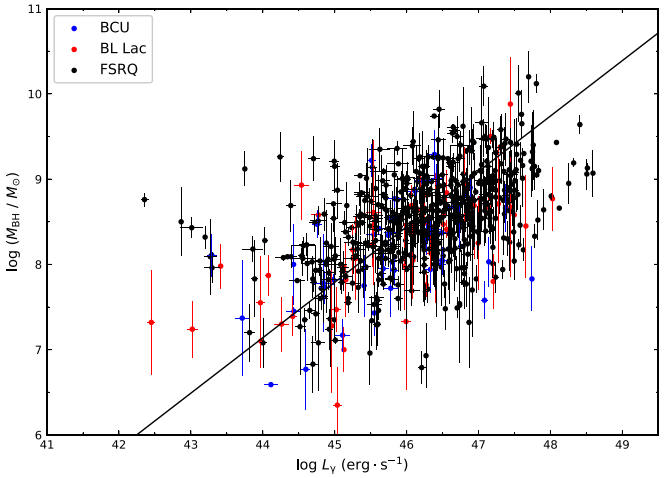

Figure 2. The correlation between BH mass and γ-ray luminosity. The black solid line stands for the result of linear regression. The blue dots stand for BCUs, red dots stands for BL Lacs, and black dots stand for FSRQs, respectively.

$\log L_\gamma = 40.38$ in unit of erg s^{-1}) than the rest of the sources due to their extreme small redshifts (0.0031 and 0.00085) with respect to the average value of their class in our sample. In addition, we also remove the BL Lac object, 4FGL J0823.3+2224 (OJ 233), for its extremely large and suspicious redshift $z = 6.443$. We suspect the redshifts of these three sources are misestimated for two possible reasons: (1) optical counterparts are wrongly associated, or (2) there are very weak emission lines on the spectrum. Linear regression is applied to analyze the correlation between γ-ray luminosity and BH mass for all the sources in our sample except for the abovementioned three. The result indicates that BH mass and γ-ray luminosity has a strong correlation from an ordinary least squares (OLS) bisector regression:

$$\log \frac{M_{\rm BH}}{M_\odot} = (0.65 \pm 0.02) \log L_\gamma - (21.46 \pm 1.04),$$

and the correlation coefficient $r = 0.52$ and the chance probability $p = 1.3 \times 10^{-44}$ are obtained through Pearson analysis. The result suggests a strong correlation between BH mass and γ-ray luminosity. Thus we suggest that γ-ray luminosity is a good BH mass estimator of blazars and propose the formula

$$\frac{M_{\rm BH}}{M_\odot} \simeq \frac{L_\gamma^{0.65}}{21.46}.$$

3.3. The Correlation between γ-ray Luminosity and BLR Luminosity

Figure 3 shows BLR luminosity as a function of γ-ray luminosity. The OLS bisector regression is employed to find a correlation between BLR luminosity and γ-ray luminosity, the result being

$$\log L_{\rm BLR} = (0.85 \pm 0.02) \log L_\gamma + (5.19 \pm 1.15).$$

Pearson partial analysis indicates an $r = 0.14$ and a $p = 5.7 \times 10^{-4}$ after removing the redshift effect from these two quantities. The result suggests that γ-ray luminosity is

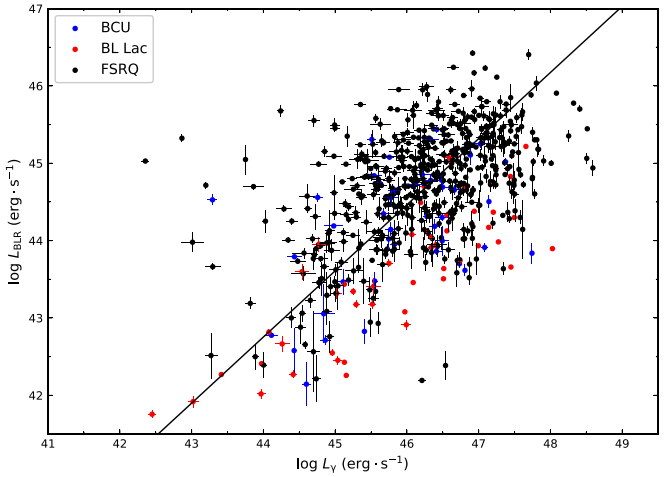

Figure 3. The correlation between BLR luminosity and γ-ray luminosity. Symbols are the same as in Figure 2.

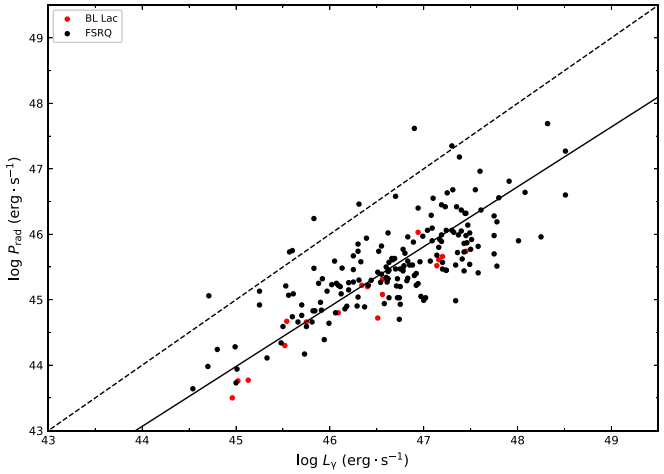

Figure 4. The correlation between jet radiation power and γ-ray luminosity. Symbols are the same as in Figure 2. The solid black line is the linear regression, and the dashed one is the equivalent line.

weakly correlated with BLR luminosity, although an apparently strong positive correlation is showing.

3.4. The Correlation between γ-ray Luminosity and Jet Radiation Power: A Lower Limit of the Doppler Factor

Figure 4 shows jet radiation power as a function of γ-ray luminosity. During the analysis, we adopt the value of $P_{\rm rad}$ from Ghisellini et al. (2014) for the common sources. OLS bisector linear regression is employed to study the correlation between jet radiation power and γ-ray luminosity for the sources in our sample. The regression result gives

$$\log P_{\rm rad} = (0.92 \pm 0.04)\log L_\gamma + (2.81 \pm 2.05),$$

with $r = 0.77$ and $p = 1.6 \times 10^{-38}$, which shows the jet radiation power is strongly correlated with γ-ray luminosity.

The blazar γ-ray emission predominates its radiation power. In fact, the L_γ should be less than both $P_{\rm rad}$ and $L_{\rm jet}^{\rm bol}$. However, there are 185 sources that lie below the equivalent line in Figure 4, showing larger L_γ than $P_{\rm rad}$. The excess of L_γ against $P_{\rm rad}$ suggests a significant Doppler-beaming effect.

We estimate a lower limit of the Doppler-beaming factor by taking two assumptions that (1) the observed γ-ray luminosity L_γ is a representative of $L_{\rm jet}^{\rm bol}$, and (2) δ equal to Γ for blazars (Zhang et al. 2020). Therefore, we have

$$\delta = \left(2f\frac{L_{\rm jet}^{\rm bol}}{P_{\rm rad}}\right)^{1/2} > \left(2f\frac{L_\gamma}{P_{\rm rad}}\right)^{1/2}.$$

The lower limit of the Doppler factor (δ) of our sources ranges from 3.0 to 48.6, with mean values for BL Lacs and FSRQs being $\delta_{\rm BL\,Lac} = 7.94 \pm 2.39$ and $\delta_{\rm FSRQ} = 11.55 \pm 6.50$; the individual values are listed in column (10) of Table 2.

4. Discussion

4.1. The Correlations

BH mass is one of the key ingredients of jet origination and radiation scenarios. There are many kinds of approaches to estimate the BH mass by using observable quantities, e.g., emission-line luminosity, absorption-line luminosity, stellar-velocity dispersion (Graham 2007; Gültekin et al. 2009; Shen et al. 2011; Shaw et al. 2012). In this work, we adopt a BH mass that is estimated by using emission lines to avoid variance between different methods; we collect the BH mass information from Paliya et al. (2021). Figure 1 shows different distributions of both $M_{\rm BH}$, because we have a 10 times larger sample of FSRQs than BL Lacs. The average values indicate that FSRQs and BL Lacs have no significant difference in their BH masses, and this may be caused by the limited number of BL Lacs in our sample. The predicted BH masses of BL Lacs should be, on average, greater than the masses of FSRQs according to the presumed "blazar cosmic evolution", in which high-power ($L_{\rm bol} > 10^{46}\,{\rm erg\cdot s^{-1}}$) blazars (mostly FSRQs) evolve to low-power blazars (mainly BL Lacs). BH mass keeps growing by accretion during the evolution (Cavaliere & D'Elia 2002; Böttcher & Dermer 2002), even though there are different opinions about it (Fan 2003).

The correlation between BH mass and γ-ray luminosity was studied by Soares & Nemmen (2020) using a sample of 154 FSRQs, and they proposed that the $M_{\rm BH}/M_\odot$ is proportional to $L_\gamma^{0.37}$. In the present work, we have a larger sample and revisit this correlation. We have confirmed the positive and strong correlation between BH mass and γ-ray luminosity for blazars as shown in Figure 2. Both Soares & Nemmen's (2020) and our results suggest blazar with more massive BH tend to have stronger γ-ray emission and to have a more powerful jet, and the power of jet will be discussed in Section 4.3. However, we have a larger slope, which is 0.65, and suggest $M_{\rm BH}/M_\odot$ proportional to $L_\gamma^{0.65}$ that indicates BH masses may grow faster with the γ-ray luminosity than they have predicted.

The correlation between L_γ and $L_{\rm BLR}$ has been performed in previous studies (Xiong & Zhang 2014; Zhang et al. 2019). This correlation proves that BLR provides seed photons for high-energy γ-rays. More importantly, it would point toward a relation between the accretion rate and the jet power (Sbarrato et al. 2012) that we will discuss in the next section.

4.2. A New Dividing Line between FSRQs and BL Lacs

The correlation between the normalized γ-ray luminosity ($L_\gamma/L_{\rm Edd}$, in Eddington units) and the normalized BLR luminosity ($L_{\rm BLR}/L_{\rm Edd}$) has been studied by Ghisellini et al. (2011) and Sbarrato et al. (2012).

$L_{\rm BLR} = \xi L_{\rm Disk}$ and $L_{\rm Disk} = \eta\dot{M}c^2$, where ξ is the photoionization coefficient, η is the energy accretion efficiency, and

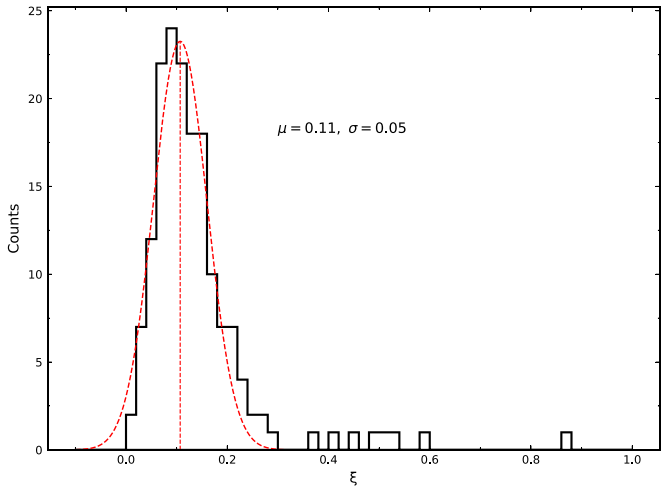

Figure 5. The distribution of ξ for the blazars. The dashed red curve stands for a Gaussian fitting of this distribution.

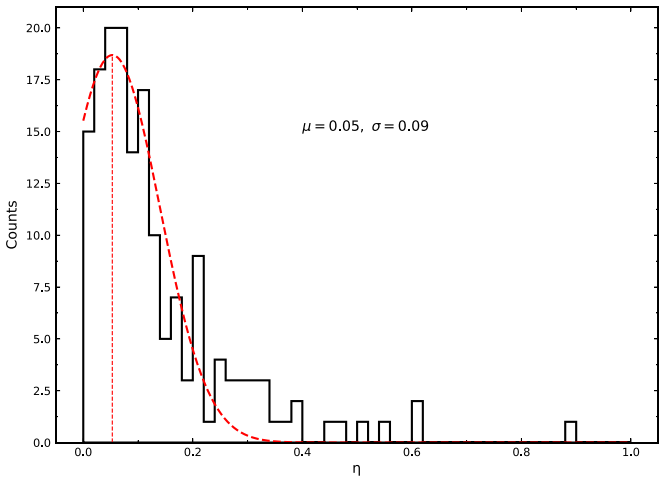

Figure 6. The distribution of η for the blazars. The dashed red curve stands for a Gaussian fitting of this distribution.

$\dot{M}$ is an accretion rate; $L_{\rm Edd} = \dot{M}_{\rm Edd}c^2$, where $\dot{M}_{\rm Edd}$ is an Eddington accretion rate. Then we can get $\frac{L_{\rm BLR}}{L_{\rm Edd}} = \xi\eta\frac{\dot{M}}{\dot{M}_{\rm Edd}}$ by substituting $L_{\rm BLR}$ and $L_{\rm Edd}$. If one holds ξ and η constant and assumes both of them to be 0.1 as former researchers did (Ghisellini et al. 2011; Sbarrato et al. 2012; Xiong & Zhang 2014), then the separation is totally determined by the $\dot{M}/\dot{M}_{\rm Edd}$, which was suggested to be 0.1 refer to $L_{\rm BLR}/L_{\rm Edd} = 1 \times 10^{-3}$ (Ghisellini et al. 2011). Later on, the value of $L_{\rm BLR}/L_{\rm Edd}$ was updated to be 5×10^{-4} (Sbarrato et al. 2012). The following study of Xiong & Zhang (2014) confirmed the idea of separation. They concluded the boundary of accretion ratio (in Eddington units) to be $\dot{M}/\dot{M}_{\rm Edd} = 0.1$, with FSRQs showing $\dot{M}/\dot{M}_{\rm Edd} > 0.1$ and BL Lacs showing $\dot{M}/\dot{M}_{\rm Edd} < 0.1$.

While we must bear in mind that η and ξ are both assumed to be 0.1 in previous studies. Here, we test the assumptions that $\xi = 0.1$ and $\eta = 0.1$ before we study the separation for blazars. ξ can be calculated with $L_{\rm BLR}$ and $L_{\rm Disk}$ for 166 sources (16 BL Lacs and 150 FSRQs) in our sample. $L_{\rm BLR}$ is obtained through emission-line properties and $L_{\rm Disk}$ is obtained from Ghisellini et al. (2014), in which they performed SED fitting to get the disk luminosity for blazars in their sample. The distribution of ξ is shown in Figure 5, a mean $\mu = 0.11$ and standard deviation $\sigma = 0.05$ are obtained when a Gaussian fitting is employed to this distribution. The η is difficult to estimate because it couples with $\dot{M}$, which is not able to measure directly. A bolometric disk luminosity can be expressed as $L_{\rm Disk} = \eta\dot{M}c^2$, which should less than $L_{\rm Edd}$. Thus, we can estimate a lower limit η because of $\eta \geqslant L_{\rm Disk}/L_{\rm Edd}$. The distribution of the η lower limit is shown in Figure 6, and the distribution gives a mean $\mu = 0.05$ and standard deviation $\sigma = 0.09$ when a Gaussian fitting is adopted to the distribution. Our distributions of ξ and η suggest that the presumed values for both ξ and η are reasonable.

Ghisellini et al. (2011) and Sbarrato et al. (2012) obtained dividing lines to separate FSRQs and BL Lacs. It is interesting to revisit the dividing line using a larger sample. We draw our sample of blazars in Figure 7 and notice many BL Lacs lying above the dividing lines that proposed by Ghisellini et al. (2011) and Sbarrato et al. (2012). Does that mean we need a new dividing line? In order to do this, we employ a support vector machine (SVM), a kind of machine-learning (ML) method, to accomplish the task of finding a new dividing line. The result of our dividing line gives an accuracy of 84.5% for the separation and is expressed as

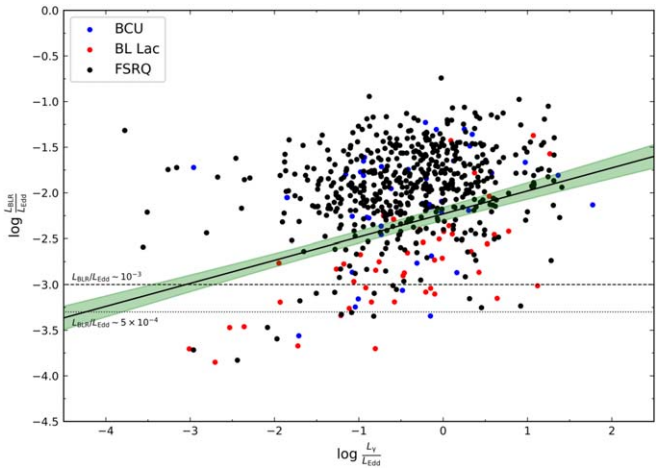

Figure 7. The correlation between normalized BLR luminosity and normalized γ-ray luminosity. Symbols are the same as in Figure 2. The solid black dividing line is our best result from the support vector machine; the green shade plot represents its 1σ error. The two horizontal lines indicate the divide between FSRQs and BL Lacs at $L_{\rm BLR}/L_{\rm Edd} \sim 10^{-3}$ from Ghisellini et al. (2011) (dashed) and at $L_{\rm BLR}/L_{\rm Edd} \sim 5 \times 10^{-4}$ from Sbarrato et al. (2012) (dotted).

$$\log\frac{L_{\rm BLR}}{L_{\rm Edd}} = 0.25\log\frac{L_\gamma}{L_{\rm Edd}} - 2.23.$$

The BL Lacs lying above the dividing line have larger accretion ratio than the BL Lacs below the line, and show consequently stronger emission from BLRs. According to the blazar evolution, we suggest these BL Lacs are at the early stage of transition from FSRQs to BL Lacs. On the contrary, the FSRQs below the dividing line have smaller accretion ratios and are at the late stage of transition. Moreover, we note that there are sources, both in the region above and the region below, that are located at the left region, $\log(L_\gamma/L_{\rm Edd}) \lesssim -2$, of the diagram. These "left-region" sources are likely to contain a broader jet and/or a misaligned jet and show the same emission-line luminosities with respect to blazars (Sbarrato et al. 2012). Abdo et al. (2010b) suggested that these "left-

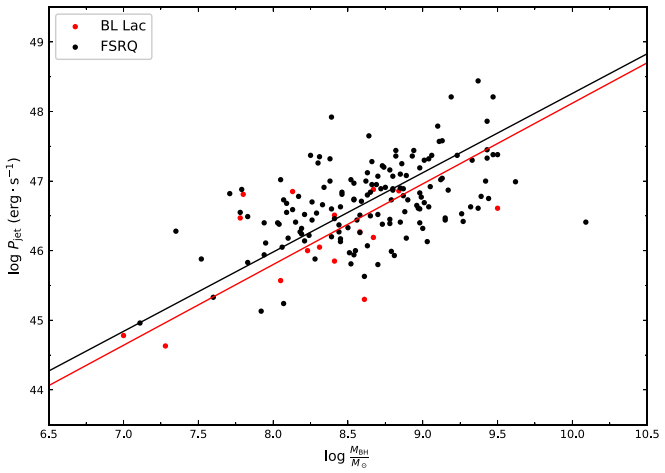

Figure 8. The correlation between entire jet power and BH mass. The meaning of different symbols are as same as Figure 2.

region" sources may be classified as radio galaxies rather than aligned blazars.

According to our result of the dividing line, we believe that $\dot{M}/\dot{M}_{\rm Edd} = 0.1$ may not be a proper criteria to separate FSRQs and BL Lacs. Instead, we suggest $\dot{M}/\dot{M}_{\rm Edd}$ evolve with the normalized γ-ray luminosity.

4.3. The Central Engine of Jets

The origin of relativistic jets is still controversial. Blandford & Znajek (BZ; 1977) used a force-free approximation and perturbative approach to study the problem of jet formation by extracting BH rotation energy. With consideration of a radiation pressure-dominated disk, one can obtain the BZ power as following:

$$L_{\rm BZ} \simeq L_{\rm Edd}\frac{f_+^2(a)f_\Omega^2(a)}{4}\left(\frac{\beta_{\rm m}}{\alpha}\right)\left(\frac{\dot{M}c^2}{L_{\rm Edd}}\right)^{-3/2}, \quad (7)$$

where $\dot{M}$ is an accretion rate, $f_+(a)$ and $f_\Omega(a)$ are dimensionless quantities at order of 1, $\beta_{\rm m}$ is a proportion that the magnetic pressure as a fraction of the total thermodynamic disk pressure near the inner disk, and α gives the disk dissipation type (see Böttcher et al. 2012). Assuming that the power through the BZ process to be entirely transformed into jets, the sum of jet kinetic power and jet radiation power, one can express jet power as

$$L_{\rm jet} \simeq L_{\rm BZ} \propto M_{\rm BH}\cdot\left(\frac{L_{\rm Disk}}{L_{\rm Edd}}\right)^{-3/2}, \quad (8)$$

which suggests that a slope of 1.0 for $\log L_{\rm jet}$ and $\log M_{\rm BH}$ and a slope of $-3/2$ for $\log L_{\rm jet}$ and $\log L_{\rm Disk}/L_{\rm Edd}$.

In order to investigate the nature of jet power, we collect $L_{\rm Disk}$, which estimated via modeling disk component with multi-temperature blackbody model in SED fitting procedure, from Ghisellini et al. (2014) and $P_{\rm jet}$, which estimated via SED fitting, from Ghisellini et al. (2014) and Tan et al. (2020). When linear regressions are used for the correlation between the jet power and BH mass, significant correlations are obtained and shown in Figure 8

$$\log P_{\rm jet} = (1.16 \pm 0.15)\log\frac{M_{\rm BH}}{M_\odot} + (36.52 \pm 1.24),$$

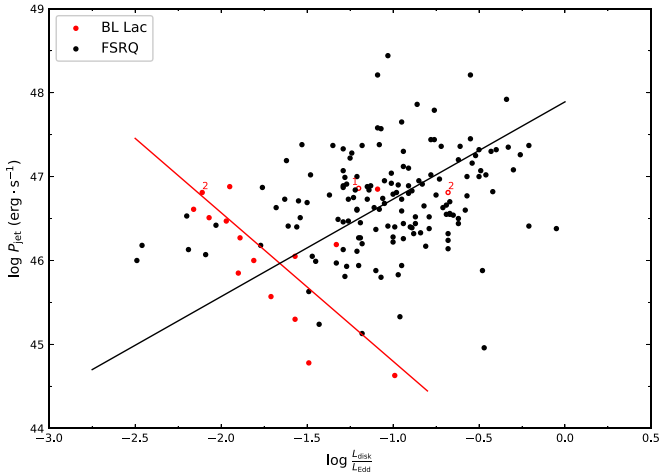

Figure 9. The correlation between the entire jet power and disk luminosity divided by the Eddington luminosity. Symbols are the same as in Figure 2. The solid lines are represented for the linear regressions for FSRQs and BL Lacs. 4FGL J0407.5+0741 and 4FGL J0438.9-4521 are marked as "1" and "2".

and $r = 0.59$ and $p = 0.02$ for BL Lacs; and

$$\log P_{\rm jet} = (1.14 \pm 0.07)\log\frac{M_{\rm BH}}{M_\odot} + (36.86 \pm 0.62),$$

and $r = 0.51$ and $p = 1.9 \times 10^{-11}$ for FSRQs. The results demonstrate strong correlations between the two quantities and suggest positive correlations between $M_{\rm BH}$ and L_γ for both BL Lacs and FSRQs. Moreover, slopes of 1.16 ± 0.15 and 1.14 ± 0.07 are consistent with the theoretically predicted slope that is 1.0 following Equation (8).

Figure 9 shows the diagram of entire jet power $P_{\rm jet}$ against normalized disk luminosity $L_{\rm Disk}/L_{\rm Edd}$. It is found that there are 2 BL Lacs in red open circles, 4FGL J0407.5+0741 and 4FGL J0438.9-4521, that are marked as "1" and "2" respectively. 4FGL J407.5+0741, known as TXS 0404+075, is a BL Lac class γ-ray emission object. However, this source is classified as FSRQs in other studies. Tan et al. (2020) suggested an external Compton model, which is usually applied to FSRQs due the existence of a BLR or a dust torus, to fit its broadband SED and studied the physical properties of FSRQs. Xiong & Zhang (2014) classified this source as a LSP, which is mostly consist of FSRQs, during their study of intrinsic γ-ray luminosity and jet power. This source shows a broad SED typical of FSRQs, but it also shows a BL Lac optical spectrum. Therefore, the exact classification of this source is in debate; it is better to exclude this source when investigating the possible physical property difference between FSRQs and BL Lacs. 4FGL J0438.9-4521 has a redshift of 2.017 and a black hole mass of $\log(M_{\rm BH}/M_\odot) = 7.8$. This black hole mass is relatively small with respect to the average values of the three classes in our sample. We note that its BH mass was obtained according to the $C_{\rm IV}(\lambda = 1549\,\mathring{A})$ emission-line profile. However, the infrared emission could be significantly absorbed by dust from the local to the galaxy itself, especially the absorption from the latter one, which can hardly be measured and compensated. We believe that the mass of this source could be underestimated due to its lower emission-line luminosity of $C_{\rm IV}$. We re-calculate the $M_{\rm BH}$ via the method that we have proposed in Section 3.2 for 4FGL J0438.9-4521 and obtain a $\log(M_{\rm BH}/M_\odot) = 9.23$. Then the plot is updated with a red dot marked as "2" with an updated BH mass. Linear regressions are

applied independently for BL Lacs and FSRQs:

$$\log P_{\rm jet} = -(1.77 \pm 0.40)\log \frac{L_{\rm Disk}}{L_{\rm Edd}} + (43.03 \pm 0.68),$$

with $r = -0.52$ and $p = 0.04$ for BL Lacs; and

$$\log P_{\rm jet} = (1.16 \pm 0.06)\log \frac{L_{\rm Disk}}{L_{\rm Edd}} + (47.89 \pm 0.62),$$

with $r = 0.27$ and $p = 8.5 \times 10^{-4}$ for FSRQs. The result of slope for BL Lac, -1.77 ± 0.40, reaches the expected slope $-3/2$ following Equation (8), indicates jets are powered by extracting BH rotation energy for BL Lacs. A positive correlation with slope 1.16 for FSRQs suggests jets power comes from at least a mixture of extracting BH rotation power and disk accretion power, and the disk accretion power may be the dominant one.

The energy extraction from BH was well established by Blandford & Znajek (1977), and the following studies suggest that this process works in blazars and radio-loud narrowline Seyfert 1 AGNs (NLS1s; Xiong & Zhang 2014; Foschini 2014). Xiong & Zhang (2014) studied the subject of blazar jet power through an investigation on the correlation between $\log L_{\rm BLR}$ and $\log P_{\rm jet}$ and obtained a slope 0.98 ± 0.07 for this correlation. Their result was perfectly consistent with the theoretically predicted slope 1 for $\log L_{\rm BLR}$ vs $\log P_{\rm jet}$ and suggested that Fermi blazar jets are powered through the BZ mechanism.

In the present work, we have confirmed that the BZ mechanism makes great efforts in Fermi blazar jet powering. Moreover, our results seem to suggest BL Lacs may be powered mostly by the BZ process of extracting energy from BH rotation. BL Lac jets are likely governed by the BH spin. However, this result should be carefully used because we only have a small sample of 16 BL Lacs with which to study the correlation between these two quantities. For FSRQs, our results suggest that their jets are powered mostly by the accretion disk. FSRQ jets rise from the inner region of accretion and the energy is transformed through the magnetic field.

4.4. Doppler-beaming Effect

Blazars are known to show extreme observation properties that are associated with the Doppler-beaming effect. The beaming effect arises from the preferential orientation of the jet, typically within $<20^\circ$ from our line of sight (Readhead et al. 1978; Blandford & Königl 1979; Readhead 1980). This effect is quantified by a Doppler factor (δ), $\delta = [\Gamma(1 - \beta\cos\theta)]^{-1}$, where Γ is the bulk Lorentz factor ($\Gamma = 1/\sqrt{1-\beta^2}$), β is the velocity of the jet in units of speed of light, and θ is the viewing angle. Since there is no direct way to measure β or θ, δ can only be estimated by indirect methods (Hovatta et al. 2009; Fan et al. 2013, 2014; Ghisellini et al. 2014; Chen 2018; Liodakis et al. 2018; Zhang et al. 2020). While different methods often yield discrepant results, Hovatta et al. (2009) and Liodakis et al. (2018) determined the variability of the Doppler factor at radio band by analyzing blazar light curves. However, the estimation at radio bands may not suitable for use in γ-ray bands. Because the γ-ray emission is extremely variable and γ-ray emission has different mechanisms, which are the synchrotron-self Compton (SSC) process and external Compton (EC) process in the leptonic scenario, compared to the radio emission mechanism, which is the synchrotron process. The Doppler factor estimation at the γ-ray band was proposed by Zhang et al. (2020); $\delta^{\rm Z20}$ can be calculated through L_γ and $L_{\rm BLR}$ for FSRQs and BL Lacs, respectively, $\log \delta^{\rm Z20}_{\rm FSRQ} = (\log L_\gamma - 1.18 \log L_{\rm BLR} + 8.00)^{0.5}$ and $\log \delta^{\rm Z20}_{\rm BL\ Lac} = (\log L_\gamma + 0.87 \log L_{\rm BLR} + 6.23)^{0.5}$.

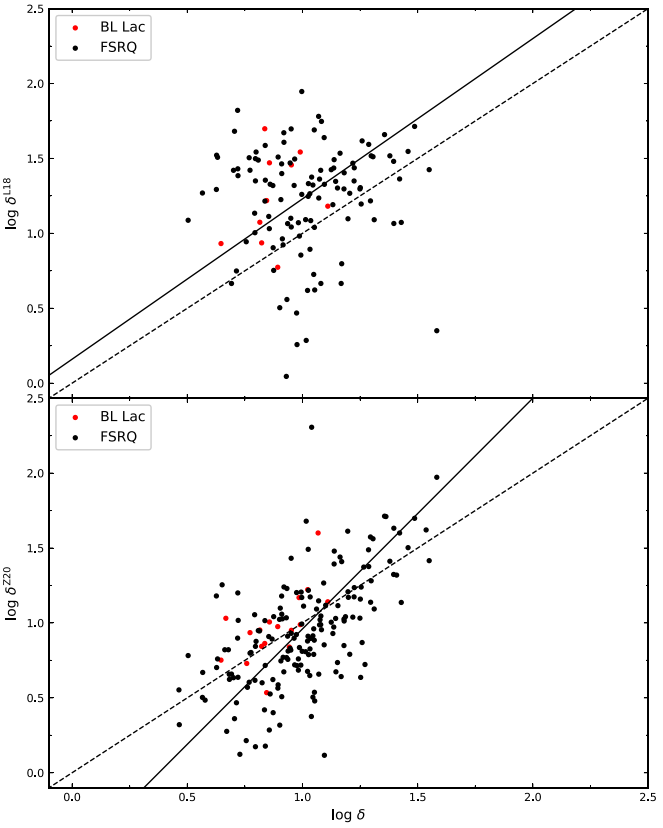

Figure 10. The comparison between the Doppler factor calculated in this work ($\log\delta$) and Doppler factors from Liodakis et al. (2018) ($\log\delta^{\rm L18}$) and from Zhang et al. (2020) ($\log\delta^{\rm Z20}$). The meaning of different symbols are as same as Figure 2. The dashed lines are the corresponding equivalent lines.

In order to make comparisons with δ which we have calculated in Section 3.4, we calculate the γ-ray Doppler factor using Zhang et al.'s (2020) method for the sources in our sample, see as $\delta^{\rm Z20}$ in Table 2 column (9). A Kolmogorov–Smirnov (K–S) test is applied to test if δ and $\delta^{\rm Z20}$ are from the same distribution. The K–S test result gives $p = 1.8 \times 10^{-14}$ that indicates δ and $\delta^{\rm Z20}$ are from two different distributions, and implies that the method we estimate δ is independent from Zhang et al.'s (2020) to estimate $\delta^{\rm Z20}$. $\delta^{\rm Z20}$ ranges from in 1.31 to 202.31 with mean values of $\langle\delta^{\rm Z20}_{\rm FSRQ} = 13.36\rangle$ and $\langle\delta^{\rm Z20}_{\rm BL\ Lac} = 11.02\rangle$. We suggest that δ and $\delta^{\rm Z20}$ are comparable for two reasons (1) the average value of $\delta^{\rm Z20}$ within the one σ error of δ, (2) the data points for the common sources are almost equally distributed below and above the equivalent line in the lower panel of Figure 10. This result is expected because these two kinds of Doppler factors are both obtained at γ-ray band and both use γ-ray luminosity.

In addition, we collect the Doppler factor from Liodakis et al. (2018); see as $\delta^{\rm L18}$ in Table 2 column (8). Similarly, a K–S test with $p = 6.3 \times 10^{-10}$ suggests δ and $\delta_{\rm L18}$ are from two different distributions, and implies that our method to estimate δ is independent from Liodakis et al.'s (2018) $\delta^{\rm L18}$ ranges from 1.11 to 88.44 with $\langle\delta^{\rm L18}_{\rm FSRQ} = 22.46\rangle$ and $\langle\delta^{\rm L18}_{\rm BL\ Lac} = 20.97\rangle$.

Among δ, $\delta^{\rm L18}$, and $\delta^{\rm Z20}$, $\delta^{\rm L18}$ has the largest average values for both FSRQs and BL Lacs. $\delta^{\rm L18}$ was derived from short-term radio variability, while $\delta^{\rm Z20}$ and δ are calculated using the 8 yr

γ-ray average flux in which the rapid variability information had been washed out. One should keep in mind that a higher variability and shorter variability timescale yield a larger Doppler factor. Consequently, $\delta^{\rm L18}$ has the largest average value among $\delta^{\rm L18}$, $\delta^{\rm Z10}$, and δ in this work.

Correlations between δ, $\delta^{\rm Z20}$, and $\delta^{\rm L18}$ for 122 common sources are shown in Figure 10. A correlation between $\log\delta$ and $\log\delta^{\rm Z20}$ suggests our lower limit for the γ-ray Doppler factor is consistent with Zhang et al.'s (2020), because we both estimate Doppler factors in the γ-ray band. However, our result is barely correlated with Liodakis et al.'s (2018) result due to different methods and wavelength bands that have been employed.

5. Conclusion

In order to study blazar jet properties and the jet central engine, in this work, we have obtained a sample of 667 Fermi blazars with available emission-line profiles, γ-ray emission, and SED information from the literature. We have studied the correlations between γ-ray luminosity and BH mass, BLR luminosity, and jet power, then further discussed accretion ratio separation of blazars, the jet origination, and proposed a new method of a lower-limit Doppler factor estimation.

Our main results are the following:

1. The analysis between BH mass and the γ-ray luminosity show a strong correlation in logarithmic space. We propose a method to estimate the BH mass from γ-ray luminosity expressed as $M_{\rm BH}/M_{\odot} \simeq L_{\gamma}^{0.65}/21.46$.
2. The correlation between BLR luminosity and γ-ray luminosity is weak. Then we normalize these two quantities with the Eddington luminosity, and generate a dividing line to separate FSRQs and BL Lacs via the ML method. The dividing line is a symbol of the accretion ratio; we suggest the accretion ratio is evolved with normalized γ-ray luminosity.
3. Through a study between jet power and BH mass, and disk luminosity, we have confirmed that the BZ mechanism works in the BH-disk system of blazars. Specifically, the BL Lac jets are likely powered mainly from extracting BH rotation energy while FSRQs jets are mostly powered by an accretion disk.
4. We propose a method of estimating a lower limit of Doppler factor using L_{γ} and $P_{\rm rad}$, give average values $\delta_{\rm FSRQ} = 11.55 \pm 6.50$ and $\delta_{\rm BL\ Lac} = 7.94 \pm 2.39$.

We are grateful for the support from our laboratory, the Key Laboratory for Astrophysics of Shanghai, and we thank Dr. Vaidehi S. Paliya for sharing data and exchanging ideas in this work. L.P.F. acknowledges the support from the National Natural Science Foundation of China (NSFC) grant No. 11933002, STCSM grant Nos. 18590780100, 19590780100, the SMEC Innovation Program 2019-01-07-00-02-E00032, and the Shuguang Program 19SG41. S.H.Z. acknowledges the support from by Natural Science Foundation of Shanghai (grant No. 20ZR1473600). J.H.F. acknowledges the support by the NSFC (NSFC 11733001, NSFC U2031201, NSFC U1531245).

ORCID iDs

Hubing Xiao https://orcid.org/0000-0001-8244-1229
Lixia Zhang https://orcid.org/0000-0003-3184-6896
Shaohua Zhang https://orcid.org/0000-0001-8485-2814
Junhui Fan https://orcid.org/0000-0002-5929-0968

References

Abdo, A. A., Ackermann, M., Agudo, I., et al. 2010a, ApJ, 716, 30
Abdo, A. A., Ackermann, M., Ajello, M., et al. 2010b, ApJ, 720, 912
Abdollahi, S., Acero, F., Ackermann, M., et al. 2020, ApJS, 247, 33
Baldwin, J. A., Wampler, E. J., & Burbidge, E. M. 1981, ApJ, 243, 76
Blandford, R. D., & Königl, A. 1979, ApJ, 232, 34
Blandford, R. D., & Payne, D. G. 1982, MNRAS, 199, 883
Blandford, R. D., & Rees, M. J. 1978, in Pittsburgh Conf. on BL Lac Objects, ed. A. M. Wolfe (Pittsburgh, PA: Univ. Pittsburgh Press), 328
Blandford, R. D., & Znajek, R. L. 1977, MNRAS, 179, 433
Böttcher, M., & Dermer, C. D. 2002, ApJ, 564, 86
Böttcher, M., Harris, D. E., & Krawczynski, H. 2012, Relativistic Jets from Active Galactic Nuclei (New York: Wiley)
Calderone, G., Ghisellini, G., Colpi, M., & Dotti, M. 2013, MNRAS, 431, 210
Cavagnolo, K. W., McNamara, B. R., Nulsen, P. E. J., et al. 2010, ApJ, 720, 1066
Cavaliere, A., & D'Elia, V. 2002, ApJ, 571, 226
Celotti, A., Padovani, P., & Ghisellini, G. 1997, MNRAS, 286, 415
Chen, L. 2018, ApJS, 235, 39
Chen, Y. Y., Zhang, X., Zhang, H. J., & Yu, X. L. 2015, MNRAS, 451 4193
Fan, J.-H. 2002, PASJ, 54, L55
Fan, J. H. 2003, ApJL, 585, L23
Fan, J.-H., Bastieri, D., Yang, J.-H., et al. 2014, RAA, 14, 1135
Fan, J.-H., Wang, Y.-J., Yang, J.-H., & Su, C.-Y. 2004, ChJAA, 4, 533
Fan, J. H., Yang, J. H., Liu, Y., et al. 2016, ApJS, 226, 20
Fan, J.-H., Yang, J.-H., Liu, Y., & Zhang, J.-Y. 2013, RAA, 13, 259
Fan, J. H., Yang, J. H., Xiao, H. B., et al. 2017, ApJL, 835, L38
Foschini, L. 2014, IJMPS, 28, 1460188
Francis, P. J., Hewett, P. C., Foltz, C. B., et al. 1991, ApJ, 373, 465
Ghisellini, G., & Tavecchio, F. 2010, MNRAS, 409, L79
Ghisellini, G., Tavecchio, F., Foschini, L., & Ghirlanda, G. 2011, MNRAS, 414, 2674
Ghisellini, G., Tavecchio, F., Maraschi, L., Celotti, A., & Sbarrato, T. 2014, Natur, 515, 376
Graham, A. W. 2007, MNRAS, 379, 711
Greene, J. E., & Ho, L. C. 2005, ApJ, 630, 122
Gültekin, K., Richstone, D. O., Gebhardt, K., et al. 2009, ApJ, 698, 198
Hovatta, T., Valtaoja, E., Tornikoski, M., & Lähteenmäki, A. 2009, A&A, 494, 527
Kaspi, S., Maoz, D., Netzer, H., et al. 2005, ApJ, 629, 61
Kaspi, S., Smith, P. S., Netzer, H., et al. 2000, ApJ, 533, 631
Kellermann, K. I., Lister, M. L., Homan, D. C., et al. 2004, ApJ, 609, 539
Liodakis, I., Hovatta, T., Huppenkothen, D., et al. 2018, ApJ, 866, 137
Lyutikov, M., & Kravchenko, E. V. 2017, MNRAS, 467, 3876
McLure, R. J., & Dunlop, J. S. 2004, MNRAS, 352, 1390
Nemmen, R. S., Georganopoulos, M., Guiriec, S., et al. 2012, Sci, 338 1445
Paliya, V. S., Domínguez, A., Ajello, M., Olmo-García, A., & Hartmann, D. 2021, ApJS, 253, 46
Pei, Z.-Y., Fan, J.-H., Liu, Y., et al. 2016, Ap&SS, 361, 237
Rani, B., Krichbaum, T. P., Fuhrmann, L., et al. 2013, A&A, 552, A11
Readhead, A. C. S. 1980, PhyS, 21, 662
Readhead, A. C. S., Cohen, M. H., Pearson, T. J., & Wilkinson, P. N. 1978, Natur, 276, 768
Sbarrato, T., Ghisellini, G., Maraschi, L., & Colpi, M. 2012, MNRAS, 421, 1764
Scarpa, R., & Falomo, R. 1997, A&A, 325, 109
Shaw, M. S., Romani, R. W., Cotter, G., et al. 2012, ApJ, 748, 49
Shen, Y., Richards, G. T., Strauss, M. A., et al. 2011, ApJS, 194, 45
Soares, G., & Nemmen, R. 2020, MNRAS, 495, 981
Tan, C., Xue, R., Du, L.-M., et al. 2020, ApJS, 248, 27
Urry, C. M., & Padovani, P. 1995, PASP, 107, 803
Urry, C. M., Scarpa, R., O'Dowd, M., et al. 2000, ApJ, 532, 816
Vestergaard, M., & Osmer, P. S. 2009, ApJ, 699, 800
Vestergaard, M., & Peterson, B. M. 2006, ApJ, 641, 689
Wandel, A., Peterson, B. M., & Malkan, M. A. 1999, ApJ, 526, 579
Wills, B. J., Wills, D., Breger, M., Antonucci, R. R. J., & Barvainis, R. 1992, ApJ, 398, 454
Woo, J.-H., & Urry, C. M. 2002, ApJ, 579, 530
Xiao, H., Fan, J., Yang, J., et al. 2019, SCPMA, 62, 129811
Xiao, H.-B., Pei, Z.-Y., Xie, H.-J., et al. 2015, Ap&SS, 359, 39
Xiong, D. R., & Zhang, X. 2014, MNRAS, 441, 3375
Zhang, L., Chen, S., Xiao, H., Cai, J., & Fan, J. 2020, ApJ, 897, 10
Zhang, L., Fan, J., & Yuan, Y. 2019, arXiv:1903.05849